Bimorph adaptive mirrors and curvature sensing

C. Schwartz, E. Ribak, and S. G. Lipson

Department of Physics, Technion—Israel Institute of Technology, Haifa 32000, Israel

The applicability of wave-front correction by means of a bimorph mirror in conjunction with a curvature sensor is described. We use Zernike polynomials to describe the quality of the atmospheric-turbulence correction analytically. The match is limited by boundary conditions of the mirror and by the discreteness of the electrodes. The correction is limited by coupling of lower- and higher-order Zernike polynomials and necessitates an interfacing computer between the wave-front sensor and the bimorph mirror.

1. INTRODUCTION

Recently considerable interest has arisen with respect to the bimorph mirror as a wave-front-correcting device coupled directly to a curvature sensor. The interest exists because of the ability of the bimorph mirror (and also of the electrostatic membrane mirror) to act as a Poisson equation solver. This research examines some practical aspects of this concept. It is concerned with the bimorph mirror but can also be applied to the membrane mirror.

As we show below, the Laplacian of the mirror surface is proportional to the local voltage. The solution of the Poisson equation and therefore the duplication of the wave front is, however, possible only if adequate boundary conditions are applied. We examine two practical aspects in particular:

a. The possibility of applying boundary conditions with only the central area of a larger bimorph mirror as the optical aperture.

b. The use of discrete electrodes, which does not permit the application of a continuous voltage distribution.

2. BIMORPH MIRROR

The bimorph mirror that interests us is made of two thin layers that are bonded together.[1] One is made of a piezoelectric material, e.g., lead zirconium titanate (PZT, which is used in this paper to indicate all similar materials), and the other is made of an optically polished material (e.g., glass or silicon). We assume that the bonding is ideal, i.e., that the adhesive is of negligible thickness and that it does not relieve any shearing stresses. A thin conducting film deposited between the two layers acts as a common electrode, and the voltage is distributed via electrodes on the back of the PZT (see Fig. 1). Another possible configuration, which is more sensitive, is constructed of two layers of PZT that are oppositely poled and are bonded together. This configuration requires a piezoelectric material that can be polished to optical quality.

When voltage is applied to the mirror, the transverse piezoelectric effect leads to a variation in the area of the PZT. The other layer of the mirror does not react, and thus spherical bending occurs, much like the linear bending of a bimetallic strip under a temperature variation.

The thickness variation is small compared with the effect on the area.

The PZT layer need not be made from a continuous sheet. It can be composed of smaller elements that are much easier to produce. The electrodes can be made to be contiguous if they are square or hexagonal. Spaces can be left between the electrodes, and spaces will also occur if the electrodes are round. The electrodes cause local bending over their area, whereas areas between the electrodes, if not fully contiguous, take a shape that is caused by their bent boundaries.

3. VOLTAGE RESPONSE

A bimorph mirror responds to a voltage distribution that is applied to it according to the following differential equation,[1] subject to adequate boundary conditions:

$$\nabla^4 Z = -A \nabla^2 V, \tag{1}$$

where $Z = Z(r, \theta)$ is the deflection of the mirror surface, $V = V(r, \theta)$ is the voltage distribution, and A is a constant that is related to the geometrical, mechanical, and piezoelectric properties of the mirror. This equation can be compared with the equation governing the bending of a thin plate under load:

$$\nabla^4 Z = \frac{q}{H}, \tag{2}$$

where $q = q(r, \theta)$ is the load intensity (force per area) and H is the rigidity factor of the plate. According to standard textbooks on elasticity,[2] we can solve Eq. (2) in two stages by solving two Poisson equations:

$$\nabla^2 M = -q, \tag{3a}$$

$$\nabla^2 Z = -\frac{M}{H}, \tag{3b}$$

$$M = \frac{M_x + M_y}{1 + \nu}, \tag{3c}$$

where $M_i = M_i(r, \theta)$ is the bending moment in direction $i = x, y$ and ν is the Poisson ratio. If we assume boundary
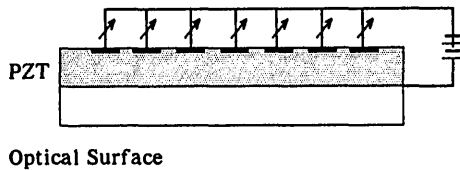
Fig. 1. Schematic drawing of a bimorph mirror. A different voltage can be applied to each electrode to control the local curvature.

conditions of a simple support, i.e., $Z = 0$ on the edge with no external moments, we obtain from Eq. (3a)

$$M = AHV,\tag{4}$$

and by using Eq. (4) in Eq. (3b) we obtain

$$\nabla^2 Z = -AV.\tag{5}$$

This differential equation, subject to the boundary conditions on Z, is of the form reached by Kokorowsky[3] and is equivalent to the equation of a membrane. The equation governing the deformation of the bimorph mirror clearly shows that the local Laplacian of the mirror surface is proportional to the local voltage.

A solution of a Poisson equation of the general form

$$\nabla^2 Z = -f(r, \theta)\tag{6}$$

in a circle of radius R with the above boundary condition ($Z = 0$) is given by[4]

$$
\begin{aligned}
Z(r,\theta) = \frac{1}{2\pi} \int_0^{2\pi} \mathrm{d}\phi \int_0^r \rho\mathrm{d}\rho \Bigg\{ &\ln\!\left(\frac{R}{r}\right) \\
&- \sum_{k=1}^{\infty} \frac{1}{k}\left(\frac{\rho^k r^k}{R^{2k}} - \frac{\rho^k}{r^k}\right) \cos[k(\phi-\theta)] \Bigg\} f(\rho,\phi) \\
+ \frac{1}{2\pi} \int_0^{2\pi} \mathrm{d}\phi \int_r^R \rho\mathrm{d}\rho \Bigg\{ &\ln\!\left(\frac{R}{\rho}\right) \\
&- \sum_{k=1}^{\infty} \frac{1}{k}\left(\frac{\rho^k r^k}{R^{2k}} - \frac{r^k}{\rho^k}\right) \cos[k(\phi-\theta)] \Bigg\} f(\rho,\phi).
\end{aligned}\tag{7}
$$

Applying a constant voltage over the entire mirror leads to a spherical surface of the form

$$Z(r) = \frac{AV}{4}(R^2 - r^2).\tag{8}$$

Using the analogy of a bimetallic plate, we can derive an expression for A with the solutions for the bending of a round bimetallic plate[5]:

$$A = \frac{12 d_{13}(t_1 + t_2)}{t_1^3 k},\tag{9a}$$

$$k = 4 + 6\left(\frac{t_2}{t_1}\right) + 4\left(\frac{t_2}{t_1}\right)^2 + \frac{E_2 t_2^3(1-\nu_1)}{E_1 t_1^3(1-\nu_2)} + \frac{E_1 t_1(1-\nu_2)}{E_2 t_2(1-\nu_1)},\tag{9b}$$

where t is the thickness, E is the Young modulus (the relevant element of the tensor), and ν, as above, is the Poisson ratio. The subscript 1 denotes the PZT, and the subscript 2 denotes the inert material. d_{13} is the transverse piezoelectric coefficient. In general, $\nu_1 \approx \nu_2 \approx 0.3$. In a simple

case, we assume that $t_1 \approx t_2 = t$ and $E_1 \approx E_2$ and obtain

$$A \approx 1.5 \frac{d_{13}}{t^2}.\tag{10}$$

The thermomechanical analogy can be applied further, and numerical calculations with thermomechanical software based on finite elements have been demonstrated.[6]

4. COUPLING THE BIMORPH MIRROR AND A CURVATURE SENSOR

A. Rigorous Treatment of the Mirror-Sensor Coupling

Let us now assume that we have a wave-front curvature sensor as proposed by Roddier[7] (actually a Laplacian sensor) that is directly coupled to the mirror without any computational stage such as was originally proposed by Roddier.[7] We perform curvature sensing by subtracting intensity distributions that are measured in two planes in front of, and behind, the focal plane. We show now that such direct coupling leads to extra correction errors that cannot be eliminated without the use of an intermediate computer. In the following discussion we ignore any sensor noise considerations.

The voltage distribution that is the output of the sensor is given by

$$
AV = \begin{cases} \nabla^2 W + \delta(\rho - a)\dfrac{\partial W}{\partial \rho} & \rho \le a \\[2mm] 0 & \rho > a \end{cases},\tag{11}
$$

where $W = W(r, \theta)$ is the measured wave-front surface and a is the radius of the optical aperture. We apply this voltage distribution to the mirror and assume that we use a small central area for the actual correction, i.e., $a \ll R$. In this way we attempt to deal with the boundary-conditions problem.[7] Here we also assume that we can apply a continuous voltage distribution. We include in A all the uniform amplification factors between the sensor and the mirror and also assume that any scale changes resulting from reimaging optics are implicit.

Neglecting smaller terms that contain R in the denominator, from Eq. (7) we obtain

$$
\begin{aligned}
Z(r,\theta) = \frac{1}{2\pi} \int_0^{2\pi} \mathrm{d}\phi \int_0^r \rho\mathrm{d}\rho \Bigg\{ &\ln\!\left(\frac{R}{r}\right) \\
&+ \sum_{k=1}^{\infty} \frac{1}{k}\left(\frac{\rho}{r}\right)^k \cos[k(\phi-\theta)] \Bigg\} \nabla^2 W \\
+ \frac{1}{2\pi} \int_0^{2\pi} \mathrm{d}\phi \int_r^a \rho\mathrm{d}\rho \Bigg\{ &\ln\!\left(\frac{R}{\rho}\right) \\
&+ \sum_{k=1}^{\infty} \frac{1}{k}\left(\frac{r}{\rho}\right)^k \cos[k(\phi-\theta)] \Bigg\} \nabla^2 W \\
+ \frac{1}{2\pi} \int_0^{2\pi} \mathrm{d}\phi\, a \Bigg\{ &\ln\!\left(\frac{R}{a}\right) \\
&+ \sum_{k=1}^{\infty} \frac{1}{k}\left(\frac{r}{a}\right)^k \cos[k(\phi-\theta)] \Bigg\} \frac{\partial W}{\partial \rho}\Bigg|_{\rho=a}.
\end{aligned}\tag{12}
$$

The form of this expression is similar to that of the solution of the Poisson equation. Let us examine it more closely. The general solution of the Poisson equa-

tion [Eq. (6)] is

$$Z(\bar{r}) = \frac{1}{4\pi} \int f(\bar{\rho}) G(\bar{r}/\bar{\rho}) \, d^2\rho$$
$$+ \frac{1}{4\pi} \int_c \left[G(\bar{r}/\bar{\rho}) \frac{\partial W}{\partial \rho} \Big|_{\rho=a} - W(a) \frac{\partial G}{\partial \rho} \Big|_{\rho=a} \right] dl, \quad (13)$$

where $G(\bar{r}/\bar{\rho})$ is a suitable Green's function.

The curvature sensor supplies us with Neumann boundary conditions. To yield a valid solution (up to an additive constant that is related to the mean deflection on the boundary), the Green's function must comply with the condition

$$\frac{\partial G}{\partial \rho} \Big|_{\rho=a} = \text{const.} \quad (14)$$

The Green's function that is embedded in Eq. (13) has the form[4] (in polar coordinates)

$$G(\bar{r}/\bar{\rho})$$
$$= \begin{cases} -2 \ln(r) + 2 \sum_{k=1}^{\infty} \frac{1}{k} \left(\frac{\rho}{r}\right)^k \cos[k(\phi - \theta)] & r > \rho \\ -2 \ln(\rho) + 2 \sum_{k=1}^{\infty} \frac{1}{k} \left(\frac{r}{\rho}\right)^k \cos[k(\phi - \theta)] & r < \rho \end{cases}. \quad (15)$$

This function has a radial derivative at the edge:

$$\frac{\partial G}{\partial \rho} \Big|_{\rho=a} = -\frac{2}{a} \left\{ 1 + \sum_{k=1}^{\infty} \left(\frac{r}{a}\right)^k \cos[k(\phi - \theta)] \right\}, \quad (16)$$

which does not comply with Eq. (14). Therefore the mirror surface duplicates the wave-front surface up to a mismatch term that has the form

$$\frac{1}{2\pi} \sum_{k=1}^{\infty} \left(\frac{r}{a}\right)^k \int_0^{2\pi} d\phi \, \cos[k(\phi - \theta)] Z(a, \phi). \quad (17)$$

This form of the mismatch calls for the use of the Zernike polynomials expansion of aberrations. The Zernike polynomials are a set of orthonormal functions in the unit circle that are suitable for the analysis of optical problems. A description of the Zernike set can be found in standard texts,[8] and their application to the problems of atmospheric propagation and adaptive optics was described in many papers.[9-11] In this study we follow the notation and the normalization convention that was introduced by Noll.[9]

For completeness we cite in Appendix A some definitions and properties that we use. Below, n denotes the radial index, and m, the azimuthal index, of the polynomials. If we introduce a wave front of the form

$$\Psi(r, \theta) = \sum_{j=1}^{\infty} a_j Z_j(r, \theta), \quad (18)$$

we can see immediately that the isotropic aberrations (i.e., those of the azimuthal order $m = 0$) are fully corrected. This makes sense, since our boundary conditions for the entire mirror ($Z = 0$) are also isotropic.

The aberrations of a higher azimuthal order induce a disturbance term of the form

$$\frac{1}{2\pi} \sum_k \int_0^{2\pi} d\phi r'^k \cos[k(\phi - \theta)] \cos(m\phi) \sqrt{2(n + 1)} \quad (19)$$

for Z_{even} and with $\sin(m\phi)$ replacing $\cos(m\phi)$ in Z_{odd}. The normalized radial coordinate is $r' \equiv r/a$. The result of the integral [relation (19)] is

$$\sqrt{\frac{(n + 1)}{2}} r'^m \cos(m\theta). \quad (20)$$

A correction of an aberration of an azimuthal order m leaves a residual aberration of the lowest radial order for that azimuthal order (for $m = 1$ tilt, for $m = 2$ astigmatism, and so on) with a factor that is related to the corrected-term radial order. This effect was previously[12] detected computationally but was not explained analytically.

We can write the correcting wave front for the mth azimuthal order as

$$\Phi_c^{(m)} = \sum_{j=i}^{\infty} a_j [Z_j^{(m)} + k_j Z_i^{(m)}], \quad (21)$$

where $Z_i^{(m)}$ is the Zernike polynomial of the aberration of the lowest radial order for the azimuthal order m (which is equal to m) and k_j is a constant that is given by

$$k_j = \begin{cases} \frac{1}{2} \left(\frac{n + 1}{m + 1}\right)^{1/2} & m > 0 \\ \left[\frac{(n + 1)}{2}\right] & m = 0 \end{cases}. \quad (22)$$

Equation (22) allows us to compute the residual mean-squared error

$$\epsilon^2 \equiv \int d^2\rho \langle (\Psi - \Phi_c)^2 \rangle w(\rho), \quad (23)$$

where $\langle \ \rangle$ denotes the ensemble average over turbulence-degraded wave fronts and $w(\rho)$ is the aperture function as defined in Appendix A. The result (see Appendix B) is

$$\epsilon^2 = \langle \Psi^2 \rangle - \sum_j \langle |a_j|^2 \rangle + \sum_{j,j'} \langle a_j a_{j'}^* \rangle k_j k_{j'}, \quad (24)$$

where $\langle \Psi \rangle$, the average of the wave-front phase, is assumed to be zero.

The terms that are included in the above sum can be calculated with the formulas that were derived by Noll.[9] Now we assume that the input wave front is degraded by atmospheric turbulence exhibiting the Kolmogorov power spectrum. We first assume an open-loop correction scheme, in which we sense the wave front and then correct it. A better approach is a closed-loop operation, in which the sensing is performed on the wave front after correction, which provides the deviations from the required wave front (see Fig. 2). The result (with no overall tilt correction) is

$$\epsilon^2 \approx 0.25 \left(\frac{D}{r_0}\right)^{5/3}. \quad (25)$$

The computation was performed up to the fourth azimuthal order; hence the approximation. $D = 2a$ is the diameter of the optical aperture, and r_0 is the turbulence-
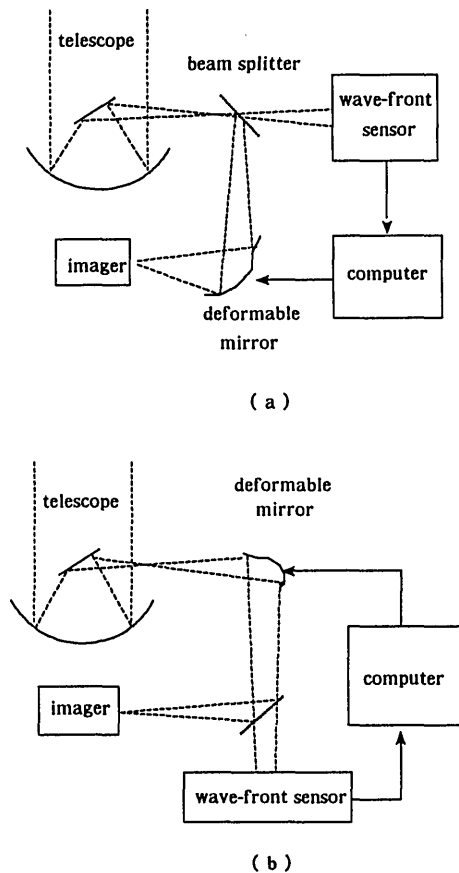
Fig. 2. (a) Open-loop adaptive-optics system (measurement of wave fronts). (b) Closed-loop operation (measurement of wave-front residuals).

coherence length defined by Fried[13] (see Appendix A). The above result is worse than just overall tilt correction, which is 0.134 $(D/r_0)^{5/3}$, but if we remove overall tilt separately the error reduces to

$$\epsilon^2 \approx 0.049 \left(\frac{D}{r_0}\right)^{5/3}, \tag{26}$$

which is dramatically better. If we now consider a closed-loop operation [see Fig. 2(b)] and assume that the control loop is much faster then the turbulence-coherence time (~10 ms at 0.5 μm), then the residual aberrations will be eliminated within the coherence time. If the feedback loop is not fast enough, then the results for the open-loop operation [relation (26)] are a good approximation.

The above results are obtained for an ideal sensor–mirror combination for which the Laplacian of the wave front can be sensed continuously and for which the measured voltages can be applied continuously over the mirror surface. This is impossible in practice, and, as we shall see in Section 5, the discreteness in sensing and voltage application introduces errors that cannot be ignored.

Let us now consider the error that results from the finite size of the mirror. There are two aberration terms. The first is

$$\frac{1}{2\pi} \int_0^{2\pi} d\phi \int_0^a \rho d\rho \left\{ \sum_{k=1}^{\infty} \frac{1}{k} \left(\frac{\rho r}{a^2}\right)^k \cos[k(\phi - \theta)] \right\} \nabla^2 W(\rho, \phi), \tag{27}$$

where W is again the measured wave-front error. This term does not contribute to the lowest radial order for each azimuthal frequency, since the Laplacian for these terms is zero.

A more substantial term (which couples high terms with low terms) is

$$\frac{1}{2\pi} \int_0^{2\pi} d\phi a \left\{ \sum_{k=1}^{\infty} \frac{1}{k} \left(\frac{\rho r}{R^2}\right)^k \cos[k(\phi - \theta)] \right\} \frac{\partial W}{\partial \rho} \bigg|_{\rho=a} . \tag{28}$$

This error, as well as the errors that we describe above, can be dealt with if we abandon the direct coupling between the curvature sensor and the bimorph mirror and add a computational stage. In this stage we determine (by numerically solving the Poisson equation) the value of the deflection on the boundary and therefore can compute a voltage distribution that should be applied to compensate for the errors that are given in expressions (19) and (28) [we neglect the error term of expression (27)].

We should take into consideration the practical limitations on the applied voltage: the maximum voltage that can be applied to the PZT without depoling it is of the order of 500–1000 V/mm. This voltage corresponds to a maximum curvature that depends on the actual parameters of the bimorph elements. The low aberrations would carry the largest amplitudes, so their correction might reach the maximum voltage. In this case the demands on the applied voltage can be somewhat alleviated if we use the area of the bimorph mirror outside the optical aperture.[14] For example, let us consider the error that is introduced by tilt that is due to the finite size of the mirror:

$$a_2 \frac{1}{2} \left(\frac{a}{R}\right)^2 r \cos(\theta), \tag{29}$$

where a_2 is the tilt (Z_2) expansion coefficient.

We can compensate for this error by applying, on the edge of the optical aperture, a voltage distribution that is proportional to $a_2(a/R)^2$. Outside the optical aperture we can apply the voltage on a circle of radius ka with a decrease in the required voltage by a factor of k^{-2}.

Note that if we do add a computational phase the curvature sensor loses some of its charm, and we can use a conventional slope sensor (such as the Hartmann–Shack sensor), even though its performance is less efficient.[14] The slope information can be used to derive both the wave front and its Laplacian.

We have assumed that the mirror is fixed on its perimeter with $Z = 0$. It is probably a demanding technical requirement, since the precision that is required is of the order of a wavelength. Errors would be insignificant for a large mirror but not for a practical one. In principle, it is possible to compensate for the mounting errors by applying voltage to the mirror at the price of a reduced dynamic range.

B. Central Support of the Mirror
Let us now consider another way of supporting the mirror. Most large astronomical telescopes are of the Cassegrain type with a central obscuration, so no correction is required in the center of the aperture. The mirror can therefore be supported on a central pole (see Fig. 3). We can use simple support boundary conditions on the inner
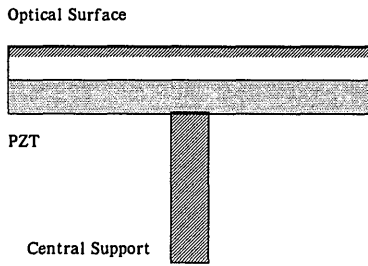
Fig. 3.   Centrally supported bimorph mirror.

boundary, whereas the outer edge is left free. The response of the mirror in this case is given by

$$
\begin{aligned}
Z(r,\theta) = \frac{1}{2\pi}\int_0^{2\pi} d\phi \int_r^R \rho d\rho & \left\{ \ln\left(\frac{1}{\rho}\right) \right.\\
& + \sum_{k=1}^{\infty} \frac{1}{k}\left(\frac{r}{\rho}\right)^k \cos[k(\phi-\theta)] \Bigg\} f(\rho,\phi)\\
& + \frac{1}{2\pi}\int_0^{2\pi} d\phi \int_{R'}^r \rho d\rho \left\{ \ln\left(\frac{1}{r}\right) \right.\\
& + \sum_{k=1}^{\infty} \frac{1}{k}\left(\frac{\rho}{r}\right)^k \cos[k(\phi-\theta)] \Bigg\} f(\rho,\phi), \qquad (30)
\end{aligned}
$$

where we have again eliminated some constant terms and some terms in which R' appears in the numerator (R' is the radius of the inner boundary; R is the outer boundary).

The output of the curvature sensor is

$$
f = AV = \begin{cases} \nabla^2 Z' + \delta(\rho-a)\dfrac{\partial W}{\partial \rho}\Big|_{\rho=a} + \delta(\rho-b)\dfrac{\partial W}{\partial \rho}\Big|_{\rho=b} & b \le \rho \le a \\ 0 & \rho < b, \rho > a \end{cases}, \quad (31)
$$

where a and b are the outer and the inner radii of the aperture.

The treatment continues in much the same way as that of the clear aperture. The difference is that the Zernike set is not orthonormal on an obscured aperture, and one should use the modified set that is described by Wang and Silva.[11] This set is less convenient for analytical treatment but can be handled numerically.

As a summary to this section we note that the error terms that arise from the inner and the outer boundaries of both the utilized aperture and the (larger) bimorph mirror can be computed and that the appropriate compensating voltage distribution can be added to the curvature-sensor output.

5. FINITE-SIZE ELECTRODES

Until now we have assumed that the voltage that is applied to the mirror has a continuous distribution. This is technically impossible, since the electrodes are of finite size. Our examination will not be fully rigorous, but it does provide some insight.

We assume that the wave-front curvature is measured spatially on a very large periodic array of sampling detectors (averaging over an area equivalent to that of a piezoelectric element) and is then reconstructed by circular piezoelectric elements. If we neglect aliasing effects and utilize the Poisson equation that is obeyed by the mirror, then we obtain from linear-systems theory

$$
k^2 \hat{Z}(\bar{k}) = k^2 \hat{W}(\bar{k})\hat{I}^2(\bar{k}), \qquad (32)
$$

where $\bar{k}$ is the spatial-frequency vector, $\hat{Z}(\bar{k})$ is the Fourier transform of the mirror deflection, $\hat{W}(\bar{k})$ is the Fourier transform of the wave-front surface, and $\hat{I}(k)$ is the Fourier transform of the sampling–reconstructing function:

$$
\hat{I}(k) = \frac{2J_1(\pi kd)}{\pi kd}, \qquad (33)
$$

with d being the diameter of the electrode.

We can eliminate k^2 from the two sides of Eq. (32) and obtain a mirror response that can be approximated by the wave front doubly convolved with the electrode shape (with the above-stated approximations). We use this relation as an approximation for a finite system. Because we neglected the influence of the boundary terms, we examine the correction of aberrations of the zeroth azimuthal order, since they are not influenced by the boundary conditions. Another approximation results because the sampling array is finite. The implications of this are discussed below.

We find in Appendix C that the correction of the nth radial order (the amount of removable rms error that is related to this order) is given by

$$
0.0046\left(\frac{D}{r_0}\right)^{5/3}(n+1)\int_0^{\infty} dk\, k^{-8/3}\left[\frac{J_{n+1}(2\pi k)}{k}\right]^2 \times \left[\frac{2J_1(2\pi k/x)}{(2\pi k/x)}\right]^4, \quad (34)
$$

where $x = D/d$ and D is the diameter of the aperture. The number of electrodes is $\sim x^2$. By assuming that the limits of integration are from zero to infinity we neglect any inner and outer turbulence-scale considerations.

As an example, we show the correction of the first isotropic aberration orders. We define the correction as the ratio of the removed wave-front error relative to the full error that is contained in each aberration order. In Fig. 4 we plot the correction of the radial orders $n = 2, 4, 6$ (the results for low x values are ignored, since we assumed a large sampling array). Similar behavior is also expected for aberrations of higher azimuthal orders. We can estimate that, for a technically achievable $x = 10$, most of the error that is contained up to the fourth order can be corrected. Therefore overall error values, which are calculated in Section 4.A, can be obtained. Subtleties concerning the boundary conditions and the shape of the electrodes array should be dealt with numerically.[12] Here we should note that aliasing effects are important because they also introduce coupling between measured high terms and induced low terms in closed-loop operation.[12] Therefore higher aberrations, which cannot be corrected by the mirror, should be filtered out.

We should stress that these results are obtained for the case of matching ordered arrays of sampling detectors and reconstructing bimorph electrodes. A geometrical configuration that is specifically designed for the correction of low-order aberrations could achieve better results with fewer electrodes.[15]
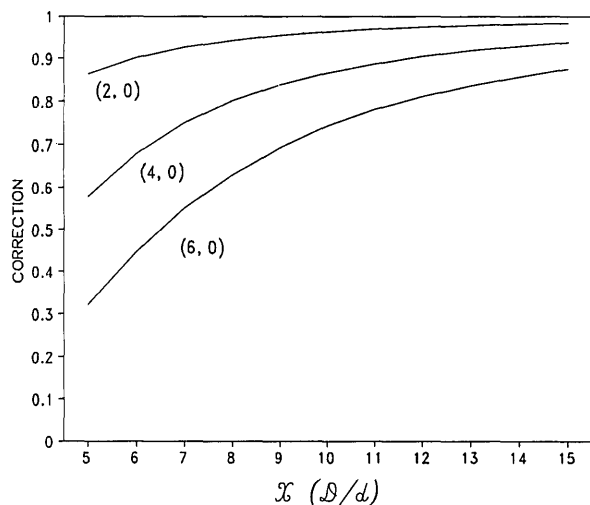
Fig. 4. Correction of the first isotropic orders (approximate treatment). x is the ratio of the optical aperture to the electrode size. The Zernike radial and azimuthal orders are denoted by (n, m). The calculation is more accurate for higher x values. The correction is drawn relative to the full correction (no aberrations) for each order.

For completeness let us consider two more configurations. One is of a single bimorph element that is tip tilted and deformed to compensate for overall defocus. The overall squared error is[9]

$$\epsilon^2 \approx 0.111 \left(\frac{D}{r_0} \right)^{5/3}. \tag{35}$$

A more complicated configuration is one in which a segmented mirror is composed of many independent bimorph elements, each of diameter d (and each of which has 3 degrees of freedom: piston, tip, and tilt). Here, following in the footsteps of Greenwood,[16] the error is given by

$$\epsilon^2 \approx 0.111 \left(\frac{d}{r_0} \right)^{5/3}. \tag{36}$$

6. CONCLUSIONS

We have discussed some practical aspects of the bimorph mirror and its possible coupling to a curvature sensor (and other sensors). It seems possible to attain a high level of correction, up to the fourth Zernike radial order, by use of a mirror with ~100 electrodes on a rectangular grid. The overall mean error can be decreased dramatically with fewer electrodes but will leave the higher-aberration orders uncorrected.

The coupling of the bimorph mirror and the curvature sensor must be supplemented by corrections to the error terms that are computed above. This is done with a computational stage between the sensor and adaptive mirror. It is also possible to use the bimorph mirror with a slope sensor because the Zernike expansion of the wave front can be easily derived from the slopes.[17] A suggested strategy is to derive the Zernike decomposition of the wave front and then to apply the appropriate voltage distribution to the mirror (including error corrections). The correction is performed up to the term that is corrected to our satisfaction.

This algorithm can be represented in the matrix form

$$\mathbf{v} = \mathbf{MDs},$$

where $\mathbf{v}$ is the vector of the voltages that are applied to the mirror electrodes, $\mathbf{s}$ is the vector of the curvature or the slope signals, $\mathbf{D}$ is the matrix that yields the Zernike expansion coefficients, and $\mathbf{M}$ is the matrix for the voltage distribution. $\mathbf{M}$ can be computed analytically with the formulas that are derived above. One performs this by using Eq. (7) and then by taking into account the need to compensate for induced errors in expressions (19) and (28). Finally, $\mathbf{MD}$ can be combined into one matrix that can be precalculated for faster application. This interaction matrix can also be measured experimentally.[14] The above research helps to clarify the source of the off-diagonal terms and thus assists us in designing better detector-bimorph electrode configurations.

APPENDIX A

Here we present some definitions and properties of the Zernike polynomials by using the notations and the normalization conventions of Noll.[9] The polynomials are defined by

$$Z_{j \text{ even}} = \sqrt{2(n + 1)} R_n^m(r) \cos(m\theta),$$

$$Z_{j \text{ odd}} = \sqrt{2(n + 1)} R_n^m(r) \sin(m\theta),$$

$$Z_j = \sqrt{(n + 1)} R_n^m(r) \quad \text{for } m = 0. \tag{A1}$$

$R_n^m(r)$ are radial polynomials based on the Jacoby polynomials:

$$R_n^m(r) = \sum_{s=0}^{(n-m)/2} \frac{(-1)^s (n - s)!}{s![(n + m)/2 - s]![(n - m)/2 - s]!} r^{n-2s}, \tag{A2}$$

where r is a normalized coordinate on the unit circle and j is an ordering index that is a function of n and m. The orthonormality relation is

$$\int_0^\infty \mathrm{d}^2 r w(r) Z_j Z_{j'} = \delta_{jj'}, \tag{A3}$$

where

$$w(r) = \begin{cases} \dfrac{1}{\pi} & r \le 1 \\ 0 & r > 1 \end{cases}.$$

The expansion of any arbitrary function that is defined inside a circle of radius R is given by

$$\Psi(R\rho, \theta) = \sum_j a_j Z_j(\rho, \theta), \tag{A4}$$

with $\rho = r/R$ and the coefficients a_j being given by

$$a_j = \int \mathrm{d}^2 \rho w(\rho) \Psi(R\rho, \theta) Z_j(\rho, \theta). \tag{A5}$$

$Q_j(k, \phi)$, the Fourier transforms of $Z_j(\rho, \theta)$, are of great im-

portance and are defined so that

$$w(\rho)Z_j(\rho, \theta) = \int d^2k\, Q_j(k, \phi)\exp(-2\pi i \bar{k} \cdot \bar{\rho}),\qquad (A6)$$

$$Q_{j\,\text{even}}(k, \phi) = \sqrt{2(n+1)}\,\frac{J_{n+1}(2\pi k)}{\pi k}(-1)^{(n-m)/2}i^m\cos(m\phi),$$

$$Q_{j\,\text{odd}}(k, \phi) = \sqrt{2(n+1)}\,\frac{J_{n+1}(2\pi k)}{\pi k}(-1)^{(n-m)/2}i^m\sin(m\phi),$$

$$Q_j(k, \phi) = \sqrt{(n+1)}\,\frac{J_{n+1}(2\pi k)}{\pi k}(-1)^{n/2}\qquad \text{for } m = 0.$$
$$(A7)$$

Now we assume a Kolmogorov power spectrum for the atmospheric turbulence[9]:

$$\hat{\Psi}(k) = 0.023 r_0^{-5/3}k^{-11/3},\qquad (A8)$$

where r_0 is Fried's coherence length, defined by

$$r_0 = 1.68\left[\left(\frac{2\pi}{\lambda}\right)^2\int dz\, C_n^2(z)\right]^{-5/3}.\qquad (A9)$$

C_n is the turbulence structure constant. Noll[9] derived correlation relations between the Zernike expansion coefficients of the atmospheric turbulence:

$$\langle a_j a_{j'}{}^* \rangle = \begin{cases} 0.1524\left(\dfrac{D}{r_0}\right)^{5/3}(-1)^{(n+n'-2m)/2}[(n+1)(n'+1)]^{1/2}\delta_{mm'} \\[4pt] \qquad \times \dfrac{\Gamma\left(\dfrac{14}{3}\right)\Gamma\left(\dfrac{n+n'-5/3}{2}\right)}{\Gamma\left(\dfrac{n-n'+17/3}{2}\right)\Gamma\left(\dfrac{n'-n+17/3}{2}\right)\Gamma\left(\dfrac{n+n'+23/3}{2}\right)} \quad j-j' \text{ even} \\[8pt] 0 \hspace{6cm} j-j' \text{ odd} \end{cases} \quad (A10)$$

The above relation contains a minor correction that was introduced by Wang and Markey.[10] The coefficients a_j are considered to be Gaussian random variables with a zero mean.

APPENDIX B

We derive an expression for the residual mean-squared error of the bimorph according to the definitions and the assumptions that are given in Section 4.A:

$$\epsilon^2 = \int d^2\rho\langle(\Psi - \Phi_c)^2\rangle w(\rho).\qquad (B1)$$

With the Zernike expansion and Eq. (21) this relation becomes

$$\epsilon^2 = \int w(\rho)d^2\rho\left\langle\left[\Psi - \sum_{j=2}^{\infty}a_j(Z_j + k_jZ_i)\right]\right.$$
$$\times\left.\left[\Psi^* - \sum_{j'=2}^{\infty}a_{j'}(Z_{j'} + k_{j'}Z_i)\right]\right\rangle$$
$$= \sigma_\Psi^2 - \int w(\rho)d^2\rho$$
$$\times\left\{\left\langle\Psi\sum_{j'=2}^{\infty}a_{j'}{}^*(Z_{j'} + k_{j'}Z_i)\right\rangle - \left\langle\Psi^*\sum_{j=2}^{\infty}a_j(Z_j + k_jZ_i)\right\rangle\right.$$
$$\left.+ \left\langle\sum_{j,j'=2}^{\infty}a_ja_{j'}{}^*(Z_jZ_{j'} + k_jZ_iZ_j + k_{j'}Z_iZ_{j'} + k_jk_{j'}Z_i^2)\right\rangle\right\},$$
$$(B2)$$

where i is the first radial order for the azimuthal order m related to the running index j. The variance of the wave front over the aperture is $\sigma_\Psi^2 = \int d^2\rho w(\rho)\Psi\Psi^*$. Using the orthonormality relations of the Zernike polynomials set and the definitions of the coefficients a_j (Appendix A), we obtain

$$\epsilon^2 = \sigma_\Psi^2 - \sum_{j=i}\langle|a_j|^2\rangle - \sum_{j=i}\langle k_j(a_j{}^*a_i + a_i{}^*a_j)\rangle$$
$$+ \sum_{j=i}\langle k_j(a_ja_i{}^*)\rangle + \sum_{j'=i}\langle k_{j'}(a_ia_{j'}{}^*)\rangle + \sum_{j,j'=i}\langle k_jk_{j'}(a_j{}^*a_j)\rangle$$
$$= \sigma_\Psi^2 - \sum_{j=i}\langle|a_j|^2\rangle + \sum_{j,j'=i}\langle k_jk_{j'}(a_j{}^*a_j)\rangle.\qquad (B3)$$

APPENDIX C

We calculate modified correlation terms between the Zernike coefficients to calculate the correction terms. We follow the procedure described by Noll.[9] The modified correlation terms are given by

$$\langle a_j{}^*a_{j'}\rangle = \int d\bar{\rho}\int d\bar{\rho}' w(\bar{\rho})w(\bar{\rho}')Z_j{}'(\bar{\rho}, \theta)C(R\bar{\rho}, R\bar{\rho}')Z_{j'}{}'(\bar{\rho}', \theta),$$
$$(C1)$$

where Z' is the aberration term that is modified by the response function. $C(R\rho, R\rho')$ is the covariance function:

$$C(R\bar{\rho}, R\bar{\rho}') = \langle\Psi(R\bar{\rho})\Psi^*(R\bar{\rho}')\rangle.\qquad (C2)$$

Equation (C1) can be written in the Fourier domain as

$$\langle a_j{}^*a_{j'}\rangle = \iint d\bar{k}d\bar{k}'Q_j{}'^*(\bar{k})\hat{\Psi}\left(\frac{k}{R'}\frac{k'}{R}\right)Q_{j'}{}'(\bar{k}'),\qquad (C3)$$

where[9]

$$\hat{\Psi}\left(\frac{k}{R'}\frac{k'}{R}\right) = 0.023\left(\frac{R}{r_0}\right)^{5/3}k^{-11/3}\delta(k - k'),\qquad (C4)$$

and the transforms of the aberration terms are modified by multiplication with the transform of the response function, i.e.,

$$Q_j{}'(k) = \sqrt{n+1}(-1)^{n/2}\frac{J_{n+1}(2\pi k)}{\pi k}\left[\frac{2J_1(2\pi k/x)}{2\pi k/x}\right]^2,\quad (C5)$$

with $x = D/d$, where D is the diameter of the aperture and d is the diameter of the electrode [see Eqs. (A7)].

We are interested in the $m = 0$ azimuthal order and with $j = j'$ terms, so the correction of the nth term is

given by

$$\langle |a_j|^2 \rangle = 0.0046 \left(\frac{D}{r_0} \right)^{5/3} (n+1) \int dk\, k^{-8/3} \left[\frac{J_{n+1}(2\pi k)}{k} \right]^2$$

$$\times \left[\frac{2J_1(2\pi k/x)}{2\pi k/x} \right]^4 . \tag{C6}$$

ACKNOWLEDGMENTS

REFERENCES

1. E. Steinhaus and S. G. Lipson, "Bimorph piezoelectric flexible mirror," J. Opt. Soc. Am. **69,** 478–481 (1979).
2. S. P. Timoshenko and S. Woinowsky-Kriger, *The Theory of Plates and Shells,* 2nd ed. (McGraw-Hill, New York, 1959), Chap. 4, Sec. 24, pp. 94–97.
3. S. A. Kokorowsky, "Analysis of adaptive optical elements made from piezoelectric bimorphs," J. Opt. Soc. Am. **69,** 181–187 (1979).
4. P. M. Morse and H. Feshbach, *Methods of Theoretical Physics* (McGraw-Hill, New York, 1953), Part 2, Chap. 10, pp. 1175–1215.
5. W. C. Young, *Roarks Formulas for Stress and Strain,* 6th ed. (McGraw-Hill, New York, 1989), Chap. 10, pp. 443–448.
6. P. Jagourel, P. Y. Madec, and M. Sechaud, "Adaptive optics: a bimorph mirror for wave front correction," in *Amplitude and Intensity Spatial Interferometry,* J. B. Breckinridge, ed., Proc. Soc. Photo-Opt. Instrum. Eng. **1237,** 394–405 (1990).
7. F. Roddier, "A new concept in adaptive optics: curvature sensing and compensation," Appl. Opt. **27,** 1223–1225 (1988).
8. M. Born and E. Wolf, *Principles of Optics,* 6th ed. (Pergamon, New York, 1980), App. VII, pp. 767–772.
9. R. J. Noll, "Zernike polynomials and atmospheric turbulence," J. Opt. Soc. Am. **66,** 207–211 (1976).
10. J. Y. Wang and J. K. Markey, "Modal compensation of atmospheric turbulence phase distortion," J. Opt. Soc. Am. **68,** 78–87 (1978).
11. J. Y. Wang and D. E. Silva, "Wave front interpretation with Zernike polynomials," Appl. Opt. **19,** 1510–1518 (1980).
12. N. Roddier and F. Roddier, "Curvature sensing and compensation: a computer simulation," in *Active Telescope Systems,* F. Roddier, ed., Proc. Soc. Photo-Opt. Instrum. Eng. **1114,** 92–96 (1989).
13. D. L. Fried, "Optical resolution through a randomly inhomogeneous medium for very long and very short exposures," J. Opt. Soc. Am. **56,** 1372–1379 (1966).
14. F. Roddier, "Wavefront curvature sensing and compensation methods in adaptive optics," in *Propagation Engineering: Fourth in a Series,* L. R. Bissonnette and W. B. Miller, eds., Proc. Soc. Photo-Opt. Instrum. Eng. **1487,** 123–128 (1991).
15. F. Roddier, M. Northcott, and J. E. Graves, "A simple low-order adaptive optics system for near-infrared applications," Publ. Astron. Soc. Pac. **103,** 131–149 (1991).
16. D. P. Greenwood, "Mutual coherence function of a wave front corrected by zonal adaptive optics," J. Opt. Soc. Am. **69,** 549–554 (1979).
17. R. Cubalchini, "Modal wave-front estimation from phase derivative measurements," J. Opt. Soc. Am. **69,** 972–977 (1979).